

Surface waves identification and extraction in a highly heterogeneous alluvial basin (Rome, Italy)

Identification et extraction des ondes de surface dans un bassin alluvial très hétérogène (Rome, Italie)

C. Varone

École Supérieure d'Ingénieurs des Travaux de la Construction (ESITC) de Paris, Arcueil, France

K. Meza Fajardo

Bureau de Recherches Géologiques et Minières (BRGM), Orléans, France

L. Lenti

French Institute of Science and Technology for Transport, Development and Networks (IFSTTAR), Marne la Vallée, France

S. Martino

University of Rome «Sapienza» and Research Center for the Geological Risks (CERI), Rome, Italy

J.F. Semblat

École Nationale Supérieure de Techniques Avancées (ENSTA) ParisTech, IMSIA, Palaiseau, France

ABSTRACT: A procedure based on the normalized inner product in the frequency-time domain has been applied to identify and extract Rayleigh surface waves from numerical seismograms composed by different typologies of seismic waves. The chosen case study is the Fosso di Vallerano area, an alluvial valley located south of the city of Rome (Italy) and characterized by a very complex geological setting due to the Tiber River depositional activity. A high-resolution engineering-geological model was reconstructed and a 2D FEM modelling has been performed to assess the local response of the valley. Prograde and retrograde Rayleigh surface waves have been identified and extracted from these computed responses. The obtained results suggest that different phenomena control the complex seismic response of the valley determining the generation of different surface waves pattern.

RÉSUMÉ : Une procédure fondée sur le produit scalaire normalisé dans l'espace temps - fréquence a été appliquée pour identifier et extraire les ondes de surface de Rayleigh à partir de sismogrammes numériques composés par plusieurs typologies d'ondes. La vallée de Vallerano, située dans la partie sud de la ville de Rome (Italie), a été choisie comme zone d'étude car elle est caractérisée par une structure géologique complexe due à l'activité de dépôt du fleuve Tibre. Un modèle géologique détaillé a été construit et deux modélisations 2D ont été exécutées afin d'évaluer la réponse sismique de la vallée par éléments finis. Des ondes de surface de Rayleigh progrades et rétrogrades ont été identifiées et extraites des réponses simulées. Les résultats obtenus suggèrent que différents phénomènes contrôlent la réponse sismique de la vallée et déterminent la génération de plusieurs contributions en ondes de surface.

Keywords: Local seismic response; Surface waves; numerical modelling; Rome.

1 INTRODUCTION

Seismic ground motions of alluvial heterogeneous basins are usually characterized by surface waves generated by the conversion of body wave energy when they propagate in the sediments (Semblat et al. 2005). Recently, Meza-Fajardo et al. 2015, 2016 proposed a time-frequency technique that allows identifying and extracting Rayleigh (prograde as well as retrograde) and Love surface waves from one-station, three-component seismograms. In the present study, the technique proposed by Meza-Fajardo et al. 2015 has been applied to identify and extract surface waves from numerical simulations on the Fosso di Vallerano valley (Rome, Italy) seismic response. More in particular, 2D numerical models have been computed by Finite Element Method (FEM) in the time domain to obtain the wave propagation all along the valley.

2 THE CASE STUDY

The Fosso di Vallerano valley is an alluvial valley located in the southern region of Rome's urban area on the left side of the Tiber River. The complex geological setting of the Fosso di Vallerano valley has been reconstructed by 250 log stratigraphies from boreholes as well as in-site geomechanical investigations, available from technical reports and official documents (Bozzano et al. 2015). Based on the data proposed by Bozzano et al. 2016, four main lithotechnical units were distinguished in the Fosso di Vallerano valley:

1. Plio-Pleistocene Marine deposits (Marne Vaticane Formation) composed by high consistency clays with silty-sandy levels;
2. Pleistocene alluvial deposits of the Paleo Tiber 4 River (650-600 ky) composed by soils including graves, sands and clays;
3. Volcanic deposits of the Alban Hills and of the Monti Sabatini Volcanic Districts

(561-360 ky) consisting of highly heterogeneous tuffs;

4. Recent alluvial deposits that filled the valley incisions since the end of the Würmian regression (18 ky-Present), characterized by a basal gravel level and including by different soft soils from sands to inorganic or peaty clays.

Mechanical and dynamic properties were attributed to each lithotechnical unit according to literature data (Bozzano et al. 2017).

The deposits composing the alluvial filling of the valley (units from 1 to 12 in Fig. 1) are characterized by Vs varying from 118 to 713 m/s. Units from 13 to 15 (Fig. 1) are characterized by Vs > 800 m/s and they represent the seismic bedrock of the area.

3 NUMERICAL MODELS

2D Numerical models along the cross sections AA' and BB' (Bozzano et al. 2016) were constructed (Fig. 1).

The numerical simulations were carried out by a Finite Element Method (CESAR-LCPC code, Humbert et al. 2005). The models have been discretized using three-noded linear elements with element size of 1 m for the alluvial filling and of 10 m for seismic bedrock for both the cross sections. A set of heterogeneous absorbing layers based on Rayleigh/Caughey damping formulation (Semblat et al. 2011) is placed at the lateral and bottom boundaries of the models to avoid spurious waves that may be reflected at the boundaries of the numerical model.

The models were excited by a 0th-order Ricker wavelet (Ricker 1943, 1953) with a PGD (Peak Ground Displacement) of 1 m and a non-negligible frequency content in the band 0.1 - 15 Hz (Fig. 2). The signal is applied at the bottom of the model at the same time in terms of horizontal and vertical displacement. Additional information about the models setting are reported in Meza-Fajardo et al., 2019.

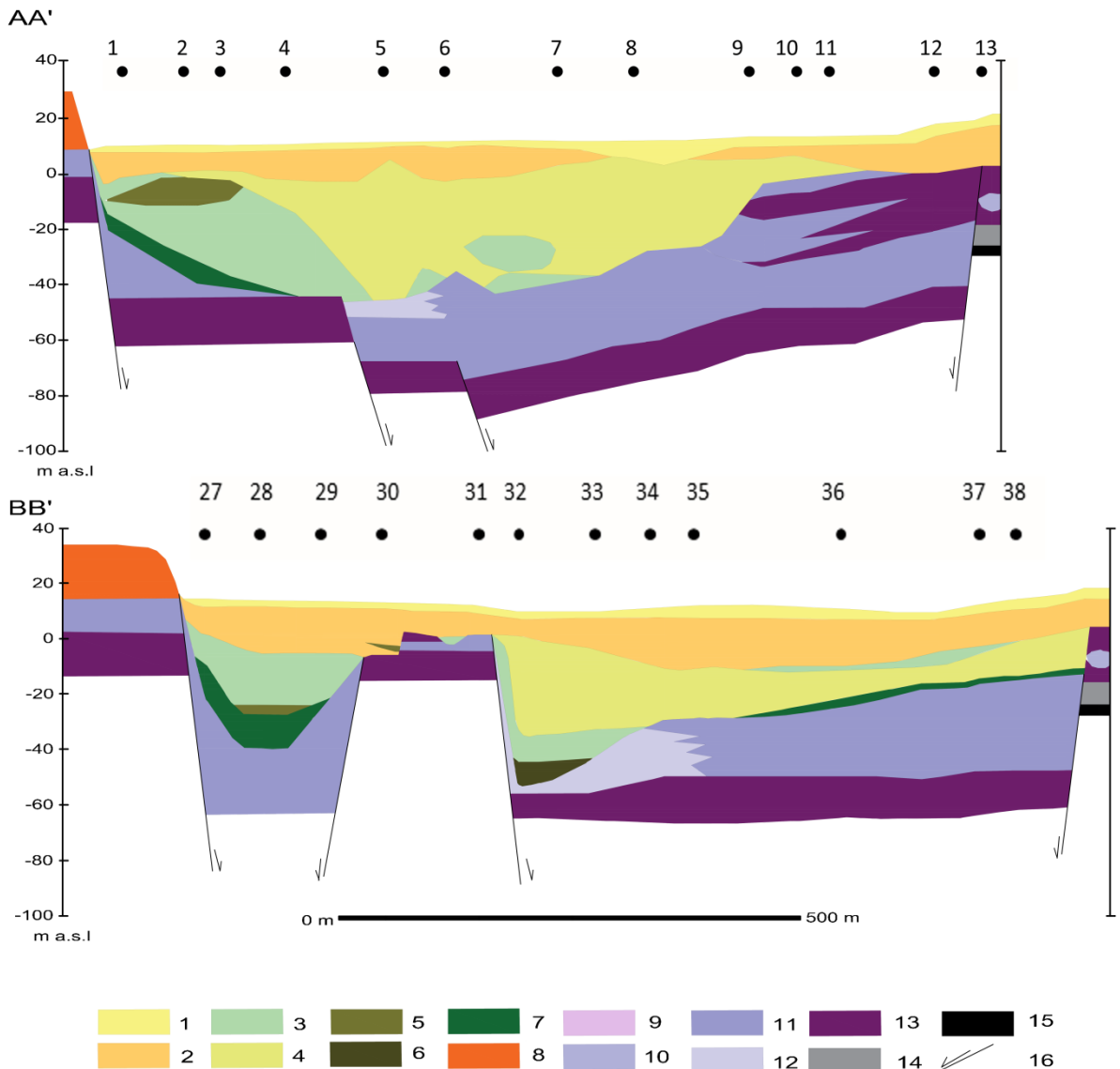


Figure 1 Geological structure of cross sections AA' and BB'. The location of the stations in which the Rayleigh waves are identified and extracted is also reported: numbers 1 to 13 (AA') and 27 to 38 (BB'). Legend of the geological cross section 1) Anthropic filling material; 2) Sandy-Clays characterized by a marked volcanic component; 3) Peaty clays, plastic; 4) Clays and silts, plastic; 5) Peat; 6) Sands and silty sands; 7) Polygenic, loose and heterometric gravels, with volcanic and sedimentary components. 8) Undifferentiated pyroclastic material; 9) Sandy clays and silts, sometimes with freshwater gastropods; 10) Clays and silts with peaty layers; 11) Sands and silty sands; 12) Loose gravels with heterometric sedimentary component; 13) Marine clays and silty clays; 14) Marine sands and silty sands; 15) Fault (modified from Bozzano et al. 2016).

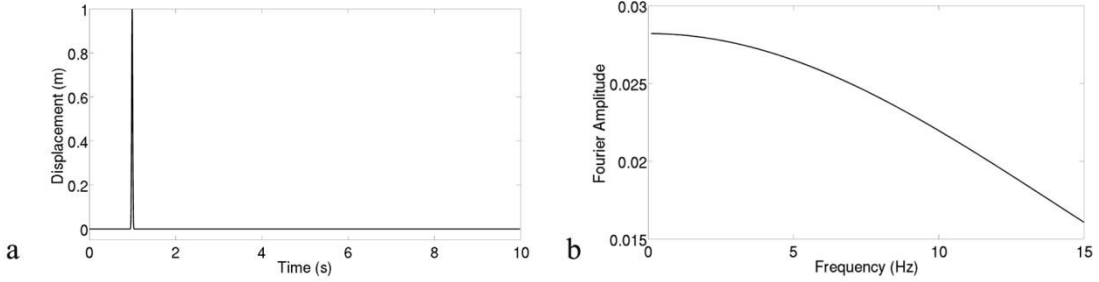


Figure 2 Time variation (a) and frequency content (b) of the Ricker wavelet applied as input in the numerical modeling.

4 IDENTIFICATION AND EXTRACTION OF SURFACE WAVES

The time-frequency technique proposed by Meza-Fajardo et al. 2015, 2016 uses the Normalized Inner Product (NIP) to identify and extract the surface waves from seismograms. The base of the method is to separate the waves by using the representation of their polarization characteristics in a time-frequency correlation. Each component of the seismogram is first resolved in the time-frequency domain by using the Stockwell Transform (Stockwell et al., 1996). The Stockwell transforms of the horizontal and vertical components of the signal, hereby named $S_H(t, f)$ and $S_V(t, f)$ respectively, may be expressed as follows (1):

$$\begin{aligned} S_c(t, f) &= \text{Re}\{S_c(t, f)\} + i \cdot \text{Im}\{S_c(t, f)\} \\ &= A_c(t, f) \exp[i \cdot \Phi_c(t, f)] \end{aligned} \quad (1)$$

Where $i = \sqrt{-1}$, $A_c(t, f)$ is the amplitude of $S_c(t, f)$ and $\Phi_c(t, f)$ is its phase.

Then, the time-frequency seismograms are filtered using the NIP to identify orthogonality between the horizontal and vertical components

since there is a phase shift of $\pm(\pi/2)$ between the horizontal and vertical components of Rayleigh waves). Performing a $\pm(\pi/2)$ shift in the vertical component S_V of the Rayleigh wave, then the resulting Transform \hat{S}_V will be in phase with the horizontal component and $NIP(S_H, \hat{S}_V) = 1$.

Then, using the relation $NIP(S_H, \hat{S}_V)$ it is possible to construct simple filters to retain only those regions in the time-frequency space in which the value of $NIP(S_H, \hat{S}_V)$ is close to 1 and setting the rest of the time-frequency space equal to zero. Finally, the time-domain horizontal and vertical components of the Rayleigh wave are obtained directly by inverting the filtered Transforms.

This technique has been here applied to the seismograms obtained at 13 stations along the AA' cross section (points from 1 to 13 Fig. 1 top) and 12 stations along the BB' cross section (points from 27 to 38 in Fig. 1 bottom).

The extracted Rayleigh waves at each station have been separated in prograde and retrograde and the obtained $NIP(S_H, \hat{S}_V)$ has been also indicated. A relation $NIP(S_H, \hat{S}_V) \geq 0.8$ represents a value of orthogonality sufficient to identify an extracted Rayleigh wave (for both prograde and retrograde waves).

5 SURFACE WAVE PATTERNS

The entire procedure has been applied to the numerical seismograms at each station and the results are presented in terms of time histories of the extracted Rayleigh waves, obtained by applying the inverse Stockwell Transform, on the records considering a minimum of $NIP(S_H, \hat{S}_V)$.

So when $NIP(S_H, \hat{S}_V) \geq 0.8$ the identified and extracted waves are Rayleigh surface waves, otherwise they could be elliptically polarized numerical noise or scattered waves.

Focusing on cross section AA' (Fig. 2) it is possible to notice that the extracted prograde

Rayleigh waves are generally speaking characterized by a $NIP(S_H, \hat{S}_V) < 0.8$. In 12 and 13 locations only this value is bigger than 0.8 so indicating that, also if these are present in the edge of the basin, a well developed pattern of “basin-induced prograde Rayleigh surface waves” is not present in the model.

On the other hand, the identified and extracted retrograde Rayleigh waves show a $NIP(S_H, \hat{S}_V) \geq 0.8$ at almost all the stations so indicating the development of a “basin-induced retrograde Rayleigh surface waves”.

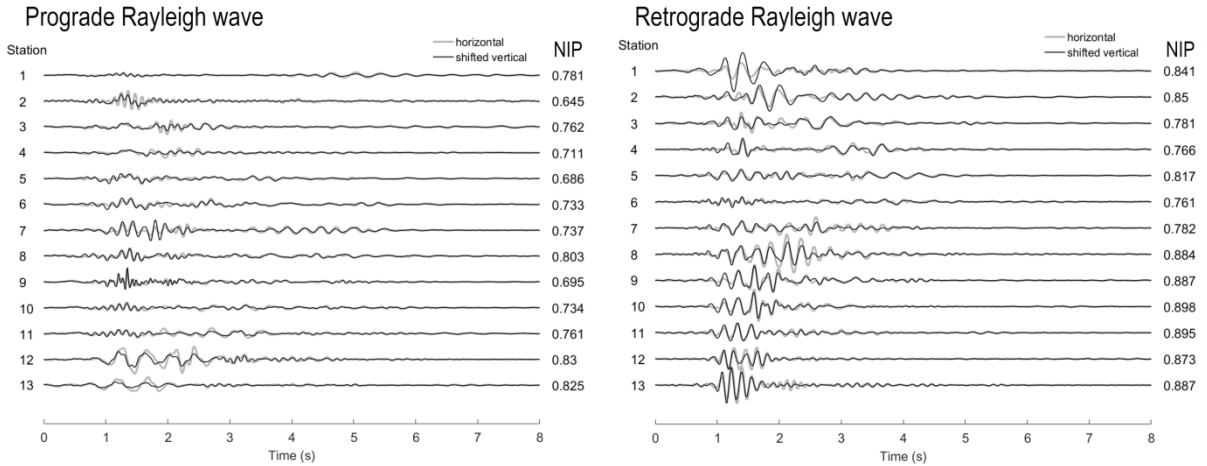


Figure 2: Horizontal and shifted vertical components of extracted Rayleigh waves on cross section AA' in Fig. 1. Prograde (left) and retrograde (right) Rayleigh surface waves are shown. See Fig. 1 for the station's location.

Moving to cross section BB' (Fig. 3) it is possible to notice that the extracted retrograde Rayleigh waves are characterized by $NIP(S_H, \hat{S}_V) \geq 0.8$ so showing a trend similar to the one presented by AA' cross section. At the same time, the prograde Rayleigh waves identified and extracted at several stations are characterized by $NIP(S_H, \hat{S}_V) \geq 0.8$. These stations are usually

located close to the edge of the basin confirming a strong control of the edge effect on the [development](#) of a “basin-induced Rayleigh surface waves” pattern. It is possible to observe that, for both AA' and BB' cross sections, the Rayleigh waves with higher amplitudes are found at the closest stations to the basin edges (Figs. 2 – 3).

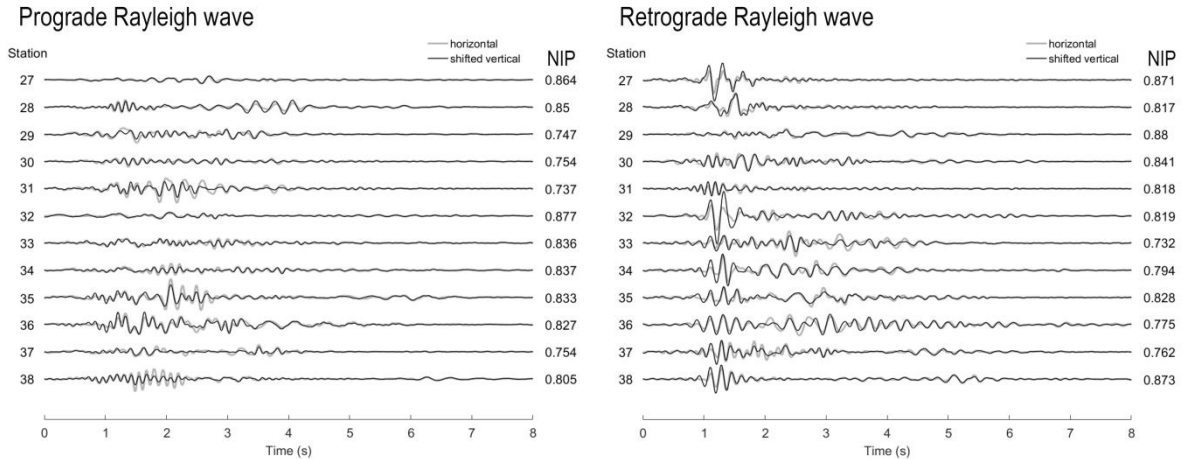


Figure 3: Horizontal and shifted vertical components of extracted Rayleigh waves on cross section BB' in Fig. 1. Prograde (left) and retrograde (right) Rayleigh surface waves are shown. See Fig. 1 for the station's location.

6 CONCLUSION

The wave propagation in the Fosso di Vallerano has been modelled applying the Finite Element Method. Two numerical models have been elaborated based on a high resolution engineering - geological model obtained by the interpolation of geotechnical and geophysical investigations.

A time-frequency technique based on the application of the Normalized Inner Product has been used to identify and extract surface waves, mainly Rayleigh waves, from numerical seismograms. The technique has been applied to identify and extract prograde and retrograde surface waves from the seismic records obtained at 25 stations distributed along two geological cross sections. Prograde waves have been observed in previous numerical simulations in basins (Malischewsky et al., 2006).

The main finding is that Finite Element simulations along with the NIP time frequency technique are effective tools to identify and extract surface waves.

Moreover, the obtained results highlight a strong influence of the basin edge effect on the generation of a "basin-induced surface waves"

pattern allowing further research focused on the relations between 2D basin effects (i.e. edge basin effect, effects due to inner heterogeneities, etc.) and the generation of surface waves in case of both synthetic as well as real ground motions.

7 REFERENCES

- Bozzano, F., Marra, F., Martino, S., Paciello, A., Scarascia Mugnozza, G., Varone, C. 2015. The local seismic response of the Fosso di Vallerano valley (Rome, Italy) based on a high resolution geological model. *Rend. Online Soc. Geol. It.*, **35**: 29-32.
- Bozzano, F., Lenti, L., Marra, F., Martino, S., Paciello, A., Mugnozza, G.S., Varone, C., 2016. Seismic response of the geologically complex alluvial valley at the "europarco business park" (rome - italy) through instrumental records and numerical modelling. *Ital J Eng Geol Environ*, **16**, 37-55. doi:10.4408/IJEGE.2016-01.O-04.
- Bozzano, F., Buccellato, A., Coletti, F., Martino, S., Marra, F., Rivellino, S., Varone, C., 2017. Analysis of the seismic site effects along the

- ancient via Laurentina (Rome). *Ann Geophys*, **60**, S0435. doi:10.4401/ag-7140.
- Humbert, P., Fezans, G., Dubouchet, A., Remaund, D., 2005 CESAR-LCPC: A computing software package dedicated to civil engineering uses. *Bullettin Lab Des Ponts Chaussée*, **256-257**, 7–37.
- Malischewsky Auning, P.G., Lomnitz, C., Wuttke, F., Saragoni, R., 2006. Prograde Rayleigh-wave motion in the valley of Mexico. *Geofísica Internacional* 45(3).
- Meza-Fajardo, K.C., Papageorgiou, A.S., Semblat, J.F. 2015. Identification and extraction of surface waves from three-component seismograms based on the normalized inner product. *Bull Seismol Soc Am*, **105**, 210-229. doi:10.1785/0120140012.
- Meza-Fajardo, K.C., Papageorgiou, 2016. Estimation of rocking and torsion associated with surface waves extracted from recorded motions. *Soil Dyn Earthq Eng*, **80**, 225-240. doi:10.1016/j.soildyn.2015.10.017.
- Meza-Fajardo K.C., Varone C., Lenti L., Martino S., Semblat J.F. 2019. Surface wave quantification in a highly heterogeneous alluvial basin: Case study of the Fosso di Vallerano valley, Rome, Italy. *Soil Dyn Earthq Eng*. doi: 10.1016/j.soildyn.2019.02.008.
- Ricker, N., 1943. Further developments in the wavelet theory of seismogram structure. *Bull. Seismol. Soc. Am.*, **33**(3), 197-228.
- Ricker, N., 1953. The form and law of propagation of seismic wavelet. *Geophysics*, **18**, 10-40.
- Semblat, J.F., Kham, M., Parara, E., Bard, P.Y., Pitilakis, K., Makra, K., Raptakis, D., 2005. Seismic wave amplification: Basin geometry vs soil layering. *Soil Dyn Earthq Eng*, **25**, 529-538.
- Semblat, J.F., Lenti, L., Gandomzadeh, A., 2011. A simple multi-directional absorbing layer method to simulate elastic wave propagation in unbounded domains. *Int. J. Numer. Meth. Eng.*, **85**, 1543-1563.
- Stockwell, R.G., Mansinha, L., Lowe, R.P., 1996. Localization of the Complex Spectrum: The S Transform. *IEEE Trans Signal Process*, **44**, 998–1001. doi:10.1109/78.492555.